© 2017. Published by The Company of Biologists Ltd | Journal of Experimental Biology (2017) 220, 1233-1244 doi:10.1242/jeb.148908

RESEARCH ARTICLE

Muscles innervated by a single motor neuron exhibit divergent synaptic properties on multiple time scales

Dawn M. Blitz‡, Amy E. Pritchard, John K. Latimer* and Andrew T. Wakefield*

ABSTRACT

Adaptive changes in the output of neural circuits underlying rhythmic behaviors are relayed to muscles via motor neuron activity. Presynaptic and postsynaptic properties of neuromuscular junctions can impact the transformation from motor neuron activity to muscle response. Further, synaptic plasticity occurring on the time scale of inter-spike intervals can differ between multiple muscles innervated by the same motor neuron. In rhythmic behaviors, motor neuron bursts can elicit additional synaptic plasticity. However, it is unknown whether plasticity regulated by the longer time scale of inter-burst intervals also differs between synapses from the same neuron, and whether any such distinctions occur across a physiological activity range. To address these issues, we measured electrical responses in muscles innervated by a chewing circuit neuron, the lateral gastric (LG) motor neuron, in a well-characterized small motor system, the stomatogastric nervous system (STNS) of the Jonah crab, *Cancer borealis*. *In vitro* and *in vivo*, sensory, hormonal and modulatory inputs elicit LG bursting consisting of inter-spike intervals of 50–250 ms and inter-burst intervals of 2–24 s. Muscles expressed similar facilitation measured with paired stimuli except at the shortest inter-spike interval. However, distinct decay time constants resulted in differences in temporal summation. In response to bursting activity, augmentation occurred to different extents and saturated at different inter-burst intervals. Further, augmentation interacted with facilitation, resulting in distinct intra-burst facilitation between muscles. Thus, responses of multiple target muscles diverge across a physiological activity range as a result of distinct synaptic properties sensitive to multiple time scales.

KEY WORDS: Augmentation, Facilitation, Central pattern generator, Neuromuscular junction

INTRODUCTION

Rhythmic behaviors are generated by the activity of multifunctional neural circuits (central pattern generators: CPGs). Higher order central nervous system inputs, sensory inputs and hormones alter the output of CPG circuits to enable adaptation to the changing internal and external environment of an organism (Briggman and Kristan, 2008; Dickinson, 2006; Doi and Ramirez, 2008; Harris-Warrick, 2011; Marder and Bucher, 2007). Motor neurons relay these changes to muscles, which generate the behaviors. However, the motor neuron to muscle transformation is often non-linear and flexible (Brezina et al., 2000; Hooper and Weaver, 2000; Hooper et al., 1999; Morris and Hooper, 1997). Thus, to fully understand how behaviors are altered by modulation of circuit activity, it is necessary to determine how muscle responses are regulated and how this may vary across a physiological range of motor neuron activity.

Muscle electrical responses are shaped by intrinsic and synaptic properties including temporal summation and activity-dependent changes in synaptic strength (Atwood, 1967; Katz et al., 1993; Sen et al., 1996; Stein et al., 2006; Zucker and Regehr, 2002). Changes in rhythmic motor neuron activity can range from the time scale of inter-spike intervals within a burst to inter-burst intervals. These time scales overlap with multiple forms of short-term plasticity that have distinct activity dependence, including depression, facilitation and augmentation (Magleby and Zengel, 1976; Martinez et al., 2014; Regehr, 2012). Persisting for hundreds of milliseconds to seconds, facilitation and depression are processes that can be induced by single action potentials, are regulated by the duration of inter-spike intervals, and enhance or decrease synaptic transmission, respectively (Regehr, 2012). Augmentation is an increase in synaptic strength which builds during sustained activity, is regulated by the duration of inter-burst intervals, and decays over tens of seconds to minutes (Deng and Klyachko, 2011; Magleby and Zengel, 1976; Regehr, 2012; Stein et al., 2006). Temporal summation, in which subsequent responses build upon previous ones that have not completely decayed, commonly occurs within bursts but can also occur across bursts in some muscles (Katz et al., 1993; Morris and Hooper, 1998; Stein et al., 2006).

From cortical to neuromuscular synapses, a neuron can express different plasticity at distinct axon terminals and thus influence multiple targets in different ways (Atwood, 1967; Blackman et al., 2013; Crider and Cooper, 2000; Davis and Goodman, 1998; Katz et al., 1993; Reyes et al., 1998; Scanziani et al., 1998). Thus far, distinctions have been identified in short-term plasticity sensitive to the timing of inter-spike intervals. However, bursting motor neuron activity occurring during rhythmic behaviors can induce the longer lasting form of plasticity known as augmentation. It has not been determined whether augmentation can also differ at distinct targets of a common motor neuron. Therefore, we tested the hypothesis that augmentation is sensitive to inter-burst intervals across a physiological range of motor neuron activity and contributes to divergent responses of multiple muscles innervated by the same motor neuron.

We explored this issue in the stomatogastric nervous system (STNS) of the Jonah crab, *Cancer borealis* Stimpson 1859. The STNS controls rhythmic movements of the crustacean foregut, including production of the gastric mill (chewing) and pyloric (filtering of food) rhythms by identified circuit neurons in the stomatogastric ganglion (STG) (Fig. 1) (Marder and Bucher, 2007; Stein, 2009). Most STG circuit neurons not only contribute to motor pattern generation but are also motor neurons. The transmitters and target muscles of these motor neurons have also been identified, and their activity has been described in response to many different

Department of Biology, Miami University, Oxford, OH 45056, USA.
*These authors contributed equally to this work

‡Author for correspondence (Dawn.Blitz@MiamiOH.edu)

D.M.B., 0000-0002-1281-6010

Received 30 August 2016; Accepted 10 January 2017

Journal of Experimental Biology (2017) 220, 1233-1244 doi:10.1242/jeb.148908

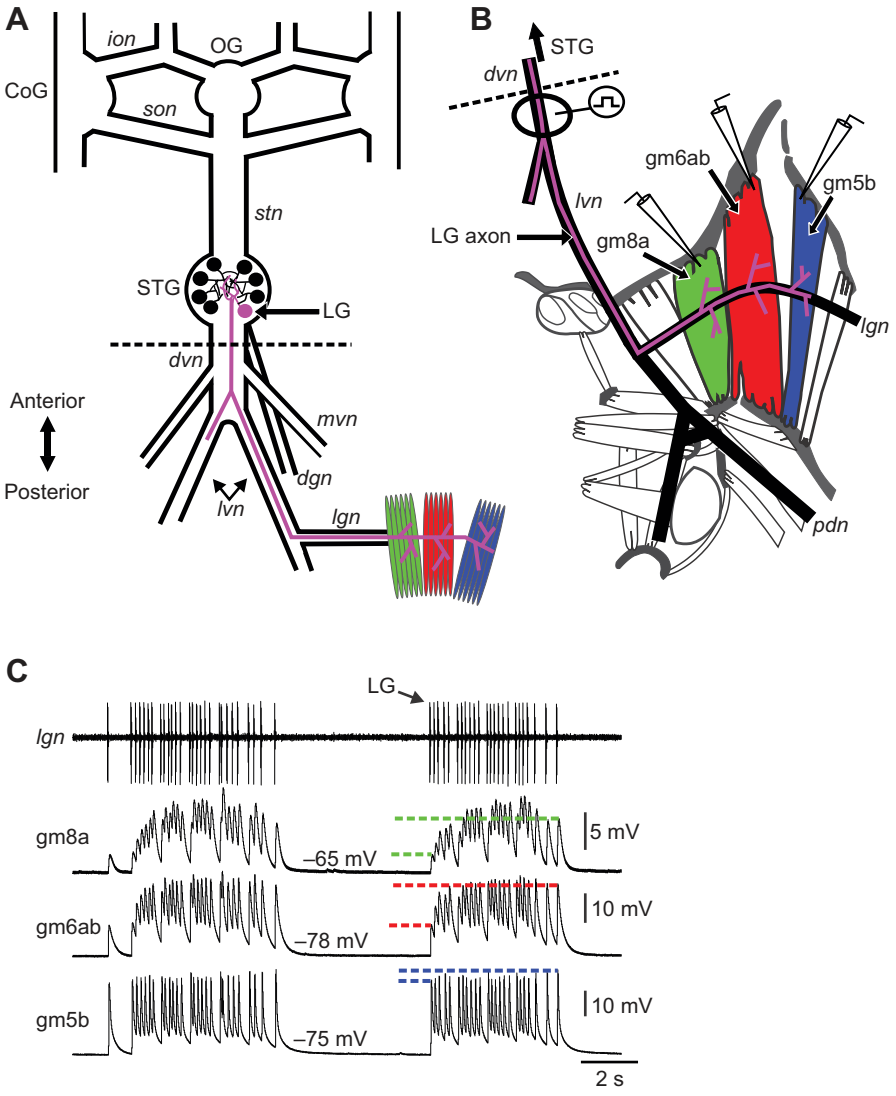

Fig. 1. Lateral gastric (LG) motor neuron provides sole innervation for three muscles in the stomatogastric nervous system (STNS). (A) Schematic diagram of the isolated STNS including LG motor neuron projection pathway and its target muscles. The complete pathway is drawn for only one side of the bilaterally symmetrical posterior region. Dashed line indicates where the dorsal ventricular nerve (*dvn*) was transected for experiments. (B) Schematic diagram of half of the posterior portion of the foregut with LG innervation of muscles gm8a, gm6ab and gm5b (Diehl et al., 2013; Weimann et al., 1991). Electrodes indicate the region of impalement of muscle fibers near their anterior insertion points. (C) Excitatory junction potential (EJP) responses of gm8a, gm6ab and gm5b to LG activity (lateral gastric nerve: *lgn*) during a triggered chewing rhythm. Despite receiving the same input from the LG neuron, there are distinct dynamics between the LG-innervated muscles. In gm8a and gm6ab at steady state, EJP_1 (lower dashed red and green lines) is smaller than other EJPs in the burst, including EJP_{last} (upper dashed red and green lines), whereas in gm5b, there is not much difference in amplitude across the burst, including EJP_1 and EJP_{last} being similar in amplitude (dashed blue lines). *ion*, inferior oesophageal nerve; *son*, superior oesophageal nerve; *stn*, stomatogastric nerve; *lvn*, lateral ventricular nerve; *mvn*, medial ventricular nerve; *dgn*, dorsal gastric nerve; *pdn*, pyloric dilator nerve. Adapted with permission from Diehl et al., 2013.

inputs (Marder and Bucher, 2007; Maynard and Dando, 1974; Nusbaum and Beenhakker, 2002; Weimann et al., 1991).

The lateral gastric (LG) motor neuron controls movements of the two lateral teeth during chewing behaviors (Diehl et al., 2013; Heinzel, 1988). LG provides the sole innervation for foregut muscles gm8a, gm6ab and gm5b (Weimann et al., 1991) (Fig. 1A,B). Like many invertebrate and lower vertebrate muscles, STNS muscles typically do not fire action potentials and have slow kinetics (Hooper et al., 1999; Jorge-Rivera et al., 1998; Weimann et al., 1997; Zhurov and Brezina, 2006; Zoccolan et al., 2002). However, 'slow' muscles vary in their ability to respond to individual action potentials and spike patterns versus the integrated spike rate of their motor neuron inputs (Daur et al., 2015; Hooper et al., 2007; Morris and Hooper, 1997, 1998; Zhurov and Brezina, 2006). Despite being slow muscles, electrical responses (excitatory junction potentials, EJPs) in the three LG targets faithfully follow multiple intra-burst patterns of LG spiking during gastric mill rhythms triggered *in vitro* and *in vivo* (Diehl et al., 2013). However, it was noted that the dynamics of LG-elicited EJPs throughout the bursts appeared different across the three LG-innervated muscles, although these differences were not examined (Fig. 1C) (Diehl et al., 2013).

Diehl et al. (2013) focused on distinctions in the pattern of spiking within LG bursts, but a number of other aspects of LG activity differ depending on modulatory state and the complement of inputs acting on LG. In response to a number of different modulatory inputs, LG activity consists of firing rates of 4–20 Hz (50–250 ms inter-spike intervals), burst durations of 2–8 s and inter-burst intervals of 2–24 s *in vitro* and *in vivo* (Beenhakker et al., 2004, 2005, 2007; Blitz et al., 2004b, 2008; Colton and Nusbaum, 2014; DeLong and Nusbaum, 2010; Diehl et al., 2013; Hedrich et al., 2011; Kirby and Nusbaum, 2007; White and Nusbaum, 2011). Similar to central and peripheral synapses in other systems, electrical responses at neuromuscular junctions in the STNS are shaped by multiple forms of activity-dependent synaptic plasticity including depression, facilitation and augmentation (Daur et al., 2012b; Jorge-Rivera et al., 1998; Katz et al., 1993; Sen et al., 1996; Stein et al., 2006). Facilitation has been identified at some LG neuromuscular synapses in *C. borealis*, and augmentation and facilitation were characterized at the LG to gm6ab synapse in *Cancer pagurus* (Jorge-Rivera et al., 1998; Sen et al., 1996; Stein et al., 2006). However, it is unknown whether there are differences in augmentation and other forms of plasticity at LG synapses onto multiple muscles in *C. borealis* that might explain distinct EJP dynamics. Thus, we examined whether there were synaptic properties contributing to distinctions in EJP dynamics and whether they are divergent at time scales of physiological intra-

Journal of Experimental Biology

Journal of Experimental Biology (2017) 220, 1233-1244 doi:10.1242/jeb.148908

burst and inter-burst LG activity parameters for the three LG-innervated muscles.

MATERIALS AND METHODS

Animals

Male wild-caught *C. borealis* crabs were obtained from commercial suppliers (Fresh Lobster, Gloucester, MA, USA; Ocean Resources, Sedgwick, ME, USA). Crabs were housed in commercial tanks containing recirculating, filtered and aerated artificial seawater (10–12°C). Crabs were maintained on a diet of thawed squid. Prior to dissection, crabs were cold anesthetized by packing in ice (30–45 min). A nerve–stomach wall preparation was dissected as previously described (Diehl et al., 2013; Weimann et al., 1991). In brief, the foregut was removed from the animal, bisected and pinned in a Sylgard 170 (Fisher Scientific, Hampton, NH, USA)-coated glass bowl in chilled *C. borealis* saline (mmol l^{-1}: 440 NaCl, 26 $MgCl_2$, 13 $CaCl_2$, 11 KCl, 10 Trizma base, 5 maleic acid; pH 7.4–7.6). Reproductive and endocrine organs and superficial fat tissue were removed. The dorsal ventricular nerve (*dvn*) and paired lateral ventricular nerves (*lvn*s) were then dissected free from surrounding tissue. The *dvn* was transected posterior to the STG, and the posterior region of the foregut cut free from the anterior portion (Fig. 1A). The nerve–stomach wall preparation was pinned in a Sylgard 184-coated Petri dish. Prior to the beginning of experiments, the fat layer overlaying the muscles was carefully removed near their anterior insertion point into ossicles to improve access for recording from muscle fibers (Fig. 1B). The foregut and nerve–stomach wall preparations were maintained in chilled saline throughout the dissection (~4°C) and subsequent experiment (8–11°C).

Electrophysiology

Stimulation of the LG axon was accomplished with an extracellular stimulation electrode. One of a pair of stainless steel wires was placed alongside the *dvn* or *lvn* nerve and a small region of the nerve and the wire was isolated with petroleum jelly (Vaseline, Amazon), with the other wire placed in the main bath compartment. Extracellular stimulation was performed with S88x stimulator and SIU-V stimulation isolation units (Natus Neurology, Warwick, RI, USA). Stimulations consisted of paired stimuli (1 ms duration, inter-stimulus intervals: 0.05, 0.1, 0.2, 0.5, 1, 2, 4, 8, 10 s; Fig. 2), or a series of repeating bursts each followed by a test pulse. Specifically, LG was stimulated in 10 consecutive bursts (1 ms stimulus duration, 4.8 s burst duration, 10 Hz intra-burst firing frequency) with a single test-EJP after each burst. The test-EJP occurred 1.5 s after the last stimulus of the burst to allow for complete decay of the final EJP in the burst (Fig. 3). This enabled measurement of the test-EJP amplitude in the absence of temporal summation as an independent measure of augmentation occurring in responses to bursts of activity. The interval between a burst+test-EJP combination and subsequent bursts was varied between 2, 4, 8, 16 and 32 s. Including the time from the end of a burst to a test-EJP, the entire duration between bursts ranged from 3.5 to 33.5 s. However, in keeping with previous literature, inter-burst intervals will refer to the duration between the test-EJP after a burst and the onset of a subsequent burst (Stein et al., 2006). The order of paired stimuli and inter-burst intervals was randomized for each set of simultaneously recorded fibers. Each paired interval was repeated three times. A full set of inter-burst intervals was performed once per fiber. At the end of running through all inter-burst intervals, the first interval in the random order was repeated, and the EJP amplitudes were compared with the first run of that interval to assess whether the quality of the recording or muscle properties changed throughout the full set of inter-burst interval stimulations. All trials had 2–3 min intervals between them to allow the muscle fiber and synapse to return to their baseline state.

Intracellular microelectrodes were made from borosilicate glass filled with 0.6 mol l^{-1} K_2SO_4 plus 10 mmol l^{-1} KCl (15–25 MΩ). Intracellular signals were amplified using Axoclamp 900A amplifiers (Molecular Devices, Sunnyvale, CA, USA) in bridge mode and digitized at ~5 kHz using a Micro 1401 data acquisition interface and Spike2 software (Cambridge Electronic Design, Cambridge, UK). Muscles were identified based on anatomical locations including ossicle insertion points (Weimann et al., 1991). The identity of gm8a was further verified by determining that fibers were only innervated by a single motor neuron when the stimulation voltage was raised (Weimann et al., 1991).

Data analysis and figure preparation

To quantify plasticity in response to paired stimuli, the paired pulse ratio (PPR: EJP_2/EJP_1) was measured. For this, the peak amplitude of the first EJP in a pair was measured relative to the baseline membrane potential prior to EJP onset. However, at some intervals there was temporal summation of the first and second EJPs. To eliminate effects of summation, an average single EJP was subtracted from the paired EJP waveform using a custom-written script in Spike 2 (freely available at http://stg.rutgers.edu/Resources.html). Specifically, single EJPs without any summation (10 s intervals) were averaged and scaled to the amplitude of the first EJP in a pair. The scaled EJP waveform was subtracted from each pair (Fig. 2A). The peak amplitude of the second EJP after subtraction was then measured from this subtracted baseline. For each fiber, the average of three sets for each interval was determined.

To assay the onset of augmentation, the amplitudes of the first EJPs per burst in 10 consecutive bursts were measured. This was repeated for each set of 10 bursts for each inter-burst interval for the three muscles. EJP_1 in $bursts_{2–10}$ was compared with EJP_1 in $burst_1$. To measure steady-state augmentation, EJP_1 was averaged across $bursts_{6–10}$. To compare steady-state augmentation between muscles, the average test-EJP amplitude after $bursts_{6–10}$ at each inter-burst interval was normalized to the average $burst_1$ test-EJP amplitude across all intervals. Interactions between facilitation and augmentation were assessed by measuring the ratio of the last EJP to the first EJP in $burst_{10}$ at all intervals.

The time constant of decay of single EJPs was determined by measuring the peak amplitude of steady-state test-EJPs and time for an EJP to decay to 37% of the peak amplitude. The influence of EJP summation in isolation from synaptic plasticity was simulated with two sequential low-pass filters with average time constants measured in each of the three muscles using a custom-written script in Spike 2 (http://stg.rutgers.edu/Resources.html) (Daur et al., 2012a; Geier and Hooper, 2002). The initial amplitudes were the same for the three simulations, but the average decay time constants for each muscle were used.

Statistical analysis was performed with SigmaPlot (Systat, San Jose, CA, USA). Parametric or non-parametric tests were used based on whether each data set to be tested was normally distributed (Shapiro–Wilk test for normality). One-sample *t*-test, repeated measures one-way ANOVA, repeated measures ANOVA on ranks, one-way ANOVA, two-way ANOVA, ANOVA on ranks, linear regression and appropriate *post hoc* tests (Tukey, Dunn's, Holm–Sidak) were used to determine statistical significance (considered as $P<0.05$) as indicated. Data are reported as means±s.e.m. In some preparations, data were collected from multiple fibers from the same

Journal of Experimental Biology (2017) 220, 1233-1244 doi:10.1242/jeb.148908

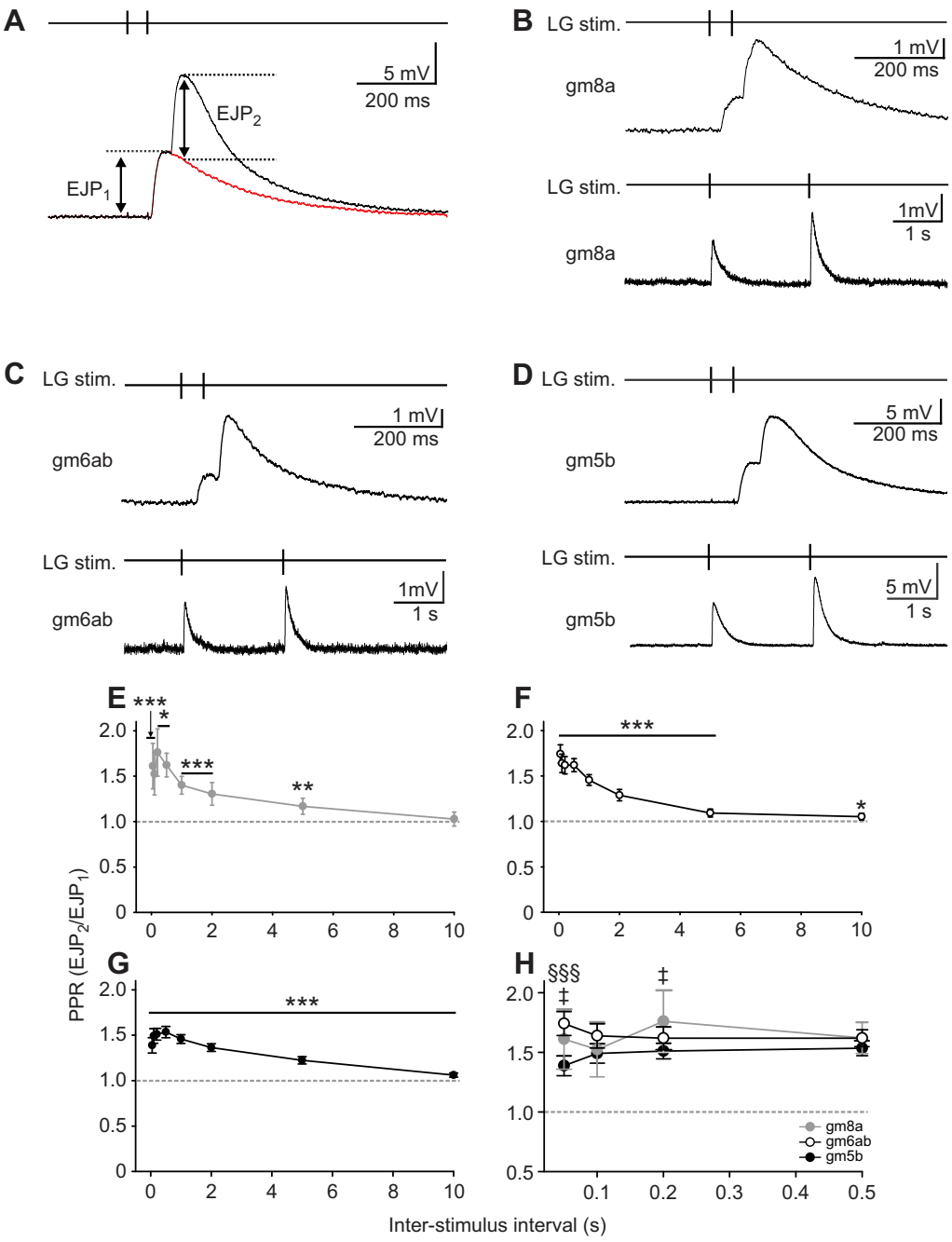

Fig. 2. Facilitation occurs in the three LG-innervated muscles. (A) At short inter-stimulus intervals, the second EJP summated with the first EJP. To measure short-term synaptic plasticity in isolation from summation effects, the average waveform of a single EJP (red) was scaled to the peak amplitude of the first EJP and subtracted to determine the baseline for the second EJP. (B–D) EJP responses to paired stimuli at 50 ms (top) and 2 s (bottom) intervals are shown for gm8a (B), gm6ab (C) and gm5b (D). LG stimulation markers are shown above all recordings. (E–G) Paired pulse ratio (PPR: EJP_2/EJP_1) versus inter-stimulus interval is plotted for gm8a (E), gm6ab (F) and gm5b (G) (means±s.e.m; one-sample *t*-test; ***P<0.001, **P<0.01, *P<0.05; all versus 1). (H) PPR versus a subset of inter-stimulus intervals (0.05–0.5 s) is plotted for gm8a, gm6ab and gm5b (two-way ANOVA, Holm–Sidak *post hoc*; ‡P<0.05 gm8a versus gm5b; §§§P<0.001 gm6ab versus gm5b). gm8a: n=7 fibers, N=3 preparations; gm6ab: n=22, N=13; gm5b: n=27, N=13.

muscle type; therefore, values are reported as n, number of fibers; N, number of preparations.

RESULTS

Facilitation/depression

The changing amplitudes of LG-elicited EJPs within bursts (LG physiological inter-spike intervals: 50–250 ms), particularly in gm6ab and gm8a (Fig. 1C), suggest that LG neuromuscular synapses could be influenced by facilitation and/or depression. Similar to many previous studies of facilitation and depression, we used paired stimuli with inter-stimulus intervals of 50 ms to 10 s to assay activity-dependent plasticity at these short time scales (Blitz et al., 2004a; Deng and Klyachko, 2011; Katz et al., 1993; Stein et al., 2006; Zucker and Regehr, 2002). To measure the amplitude of the second EJP without the influence of summation, the waveform of a single EJP was aligned to the first EJP and subtracted from the response to two stimuli (see Materials and methods) (Fig. 2A).

We found that EJPs in all three muscles were influenced by some degree of facilitation. At 50 ms, the second EJP summated with the first EJP in the three muscles (Fig. 2B–D, top). Additionally, the amplitude of the second EJP independent of summation was larger than the amplitude of the first, although there was greater facilitation in the second EJP at 50 ms in gm8a and gm6ab compared with gm5b. With a 2 s interval, there was no summation but the second EJP was still larger than the first EJP, to a similar extent in all three muscles (Fig. 2B–D, bottom). Plotting the average PPR across preparations, there was facilitation (PPR>1) at most intervals from 50 ms to 10 s in the three muscles (Fig. 2E–G, Table 1). The plots of paired pulse plasticity diverged at the shortest inter-stimulus interval (50 ms), with greater facilitation in gm8a and gm6ab than in gm5b

Journal of Experimental Biology (2017) 220, 1233-1244 doi:10.1242/jeb.148908

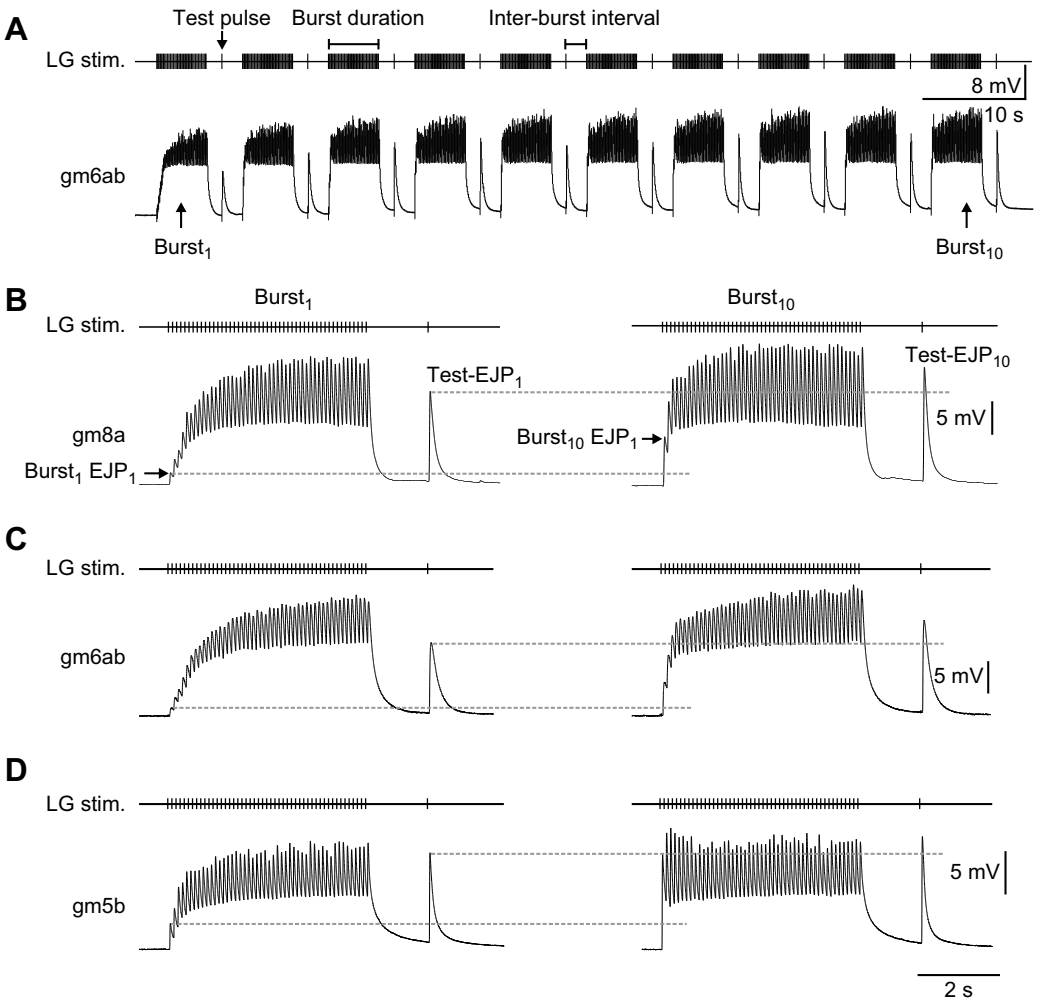

Fig. 3. Augmentation occurs in three LG-innervated muscles. (A) The stimulation protocol to measure augmentation consisted of a 4.8 s burst with an intra-burst frequency of 10 Hz followed by a single test pulse, repeated 10 times. The intervals between the burst+test pulse and the following burst varied between 2 and 32 s. $Burst_1$ and $burst_{10}$ for gm8a (B), gm6ab (C) and gm5b (D) highlight changes that occur over the course of 10 bursts with an 8 s inter-burst interval. Dashed gray lines indicate the peak amplitude of $burst_1$ EJP_1 (lower line in each set) and the peak amplitude of $burst_1$ test-EJP_1 (upper line in each set). LG stimulation markers are shown above each recording.

(Fig. 2H, Table 2). This could reflect a longer time necessary for facilitation to fully develop at the LG to gm5b synapses or an interaction of facilitation and depression (Dittman et al., 2000; Dobrunz et al., 1997; Regehr, 2012) (see also 'Interactions between facilitation and augmentation' below).

Augmentation

In addition to facilitation and depression acting on a short (milliseconds to seconds) time scale, many synapses also express augmentation acting on a longer time scale (minutes). The rhythmic bursting activity of LG during gastric mill rhythms is typical of

Table 1. Statistical analyses of individual muscles

	gm8a			gm6ab			gm5b		
	n	*N*	Significance	*n*	*N*	Significance	*n*	*N*	Significance
Facilitation:									
PPR	7	3	[a]**Yes**; Fig. 2	22	13	[a]**Yes**; Fig. 2	27	13	[a]**Yes**; Fig. 2
Augmentation:									
$Bursts_{2–10}$ EJP_1 vs $burst_1$ EJP_1	9	4	[b,c]**Yes**; Fig. 4	12	6	[b,c]**Yes**; Fig. 4	14	6	[b,c]**Yes**; Fig. 4
EJP_1 across $bursts_{6–10}$	9	4	[b,d]*P*=0.46–1.0	12	6	[b,d]*P*=0.31–1.0	14	6	[d]*P*=0.95–1.0
$Burst_{6–10}$ EJP_1 between intervals	9	4	[b]**Yes**; Fig. 4	12	6	[b]**Yes**; Fig. 4	14	6	[d]**Yes**; Fig. 4
Test-$EJP_{6–10}$ vs test-EJP_1	9	4	[b]**Yes**; Fig. 5A	12	6	[b]**Yes**; Fig. 5A	14	6	[c]**Yes**; Fig. 5A
Intra-burst facilitation:									
EJP_{last}/EJP_1	9	4	[a]**Yes**; Fig. 7	12	6	[a]**Yes**; Fig. 7	14	6	[a]**Yes**; Fig. 7
EJP_{last}/EJP_1 vs inter-burst interval	9	4	[e]r^2=0.56	12	6	[e]r^2=0.76	14	6	[e]r^2=0.64

PPR, paired-pulse ratio; *n*, number of fibers; *N*, number of preparations. [a]One-sample *t*-test; [b]one-way repeated measures ANOVA, Holm–Sidak *post hoc*; [c]repeated measures ANOVA on ranks, Dunn's *post hoc*; [d]repeated measures ANOVA on ranks, Tukey *post hoc*; [e]linear regression. Bold indicates significance. Detailed statistical results across inter-spike intervals, inter-burst intervals or burst number are given in the cited figures.

Journal of Experimental Biology (2017) 220, 1233-1244 doi:10.1242/jeb.148908

Table 2. Statistical comparisons between muscles

	gm8a		gm6ab		gm5b		Comparison		
	n	*N*	*n*	*N*	*n*	*N*	gm8a vs gm6ab	gm8a vs gm5b	gm6ab vs gm5b
Facilitation: PPR	7	3	22	13	27	13	[a]*P*=0.733	[a]**Yes**; Fig. 2	[a]**Yes**; Fig. 2
Baseline: $burst_1$ EJP_1	9	4	12	6	14	6	[b]*P*=1.0	[b]***P*<0.001**	[b]***P*<0.001**
Augmentation: normalized test-EJP amplitude	9	4	12	6	14	6	[a]**Yes**; Fig. 5B	[a]**Yes**; Fig. 5B	[a]**Yes**; Fig. 5B
Intra-burst facilitation: Ratio EJP_{last}/EJP_1	9	4	12	6	14	6	[a]*P*=0.14–0.86	[a]**Yes**; Fig. 7	[a]**Yes**; Fig. 7
Summation: decay τ	9	4	17	11	19	11	[b]*P*=1.0	[b]***P*<0.001**	[b]***P*<0.001**

PPR, paired-pulse ratio; *n*, number of fibers; *N*, number of preparations. [a]Two-way ANOVA, Holm–Sidak *post hoc*; [b]ANOVA on ranks, Dunn's *post hoc*. Bold indicates significance. Detailed statistical results across inter-spike intervals, inter-burst intervals or burst number are given in the cited figures.

activity that elicits augmentation, and augmentation does in fact shape gm6ab responses to LG activity in *C. pagurus* (Stein et al., 2006). Distinct inputs elicit LG bursting with different inter-burst intervals. Therefore, we asked whether EJP amplitudes in gm8a, gm6ab and gm5b in *C. borealis* differ across a range of inter-burst intervals, due to differences in augmentation. Our protocol was similar to the one used to characterize augmentation in gm6ab in *C. pagurus* with some quantitative differences (Stein et al., 2006) (see Materials and methods) (Fig. 3A). In all three muscles, the amplitudes of EJP_1 within bursts and test-EJPs after the bursts increased with repeated bursts. For instance, in response to bursts with an inter-burst interval of 8 s, EJP_1 was larger in $burst_{10}$ than in $burst_1$ in gm8a (Fig. 3B), gm6ab (Fig. 3C) and gm5b (Fig. 3D) (dashed gray lines). Similarly, test-EJP_{10} was larger than test-EJP_1 in all three muscles (Fig. 3B–D). Thus, EJPs in all three muscles are shaped by augmentation. We next determined whether there were differences in augmentation across the muscles.

To determine how changes in EJP amplitude developed during repetitive bursts, we quantified the amplitude of EJP_1 in $burst_1$ through to $burst_{10}$. At baseline there were differences in the amplitude of the first EJP ($burst_1$, EJP_1) when there was no stimulation for at least 2 min. EJP_1 was larger in gm5b (6.0 ±0.7 mV) than in gm8a (1.2±0.2 mV) and gm6ab (1.2±0.1 mV), which were not different from each other (Table 2). For all three muscles, the amplitude of EJP_1 increased over the first several LG bursts. The increase was significant by $burst_2$–$burst_5$ (Fig. 4, indicated to the right of plots) for inter-burst intervals of 2–32 s for all three muscles (Fig. 4, Table 1). To determine whether there were differences in the relative amounts of augmentation at different inter-stimulus intervals, we assayed steady-state augmentation. Because there was no difference in the amplitude of EJP_1 across $burst_6$ to $burst_{10}$ at all inter-burst intervals (Table 1), the average EJP_1 amplitude for $burst_{6–10}$ was measured as the steady-state augmented amplitude for each inter-burst interval. We found similar $burst_{6–10}$ EJP_1 amplitudes between longer inter-burst intervals (32 versus 16 s and 16 versus 8 s) in gm8a (Fig. 4A, brackets to the right of plots; Table 1). However, $burst_{6–10}$ EJP_1 amplitude in gm8a was greater at 4 versus 8 s intervals but again not different between 4 and 2 s intervals. In gm6ab, $burst_{6–10}$ EJP_1 amplitude did not differ between 32 and 16 s intervals but was greater with increasingly shorter intervals from 16 to 2 s (8 versus 16, 4 versus 8 and 2 versus 4 s) (Fig. 4B, Table 1). In gm5b, the $burst_{6–10}$ EJP_1 amplitude was greater at 8 s than at 16 s, but was not different between 4 and 8 s or 2 and 4 s inter-burst intervals or between 32 and 16 s (Fig. 4C, Table 1). Thus, another distinction between the muscles was that augmentation saturated at 8 s inter-burst intervals in gm5b, but at shorter intervals in gm8a (4 s) and gm6ab (2 s).

To further compare the sensitivity of synaptic responses to burst stimulations, we quantified changes in test-EJPs for the three muscles. The average test-EJP_1 amplitudes for each muscle were plotted, followed by the average test-$EJP_{6–10}$ amplitudes for each inter-burst interval (Fig. 5A). In all three muscles, the test-$EJP_{6–10}$ amplitude was greater than the test-EJP_1 amplitude at inter-burst intervals of 2–16 s, and also greater than the test-EJP_1 amplitude at 32 s intervals in gm6ab and gm8a (Fig. 5A, Table 1). Although test-EJP amplitudes were greater in gm5b than in the other muscles, when the test-$EJP_{6–10}$ amplitudes were normalized to test-EJP_1, greater augmentation was evident in gm8a and gm6ab than in gm5b (Fig. 5B, Table 2). The saturation of augmentation at 8 s in gm5b is also illustrated in the plot of normalized gm5b test-EJP amplitudes as the plot is flat between 2 and 8 s. Thus, in addition to saturation at different intervals, there are differences between the muscles in the extent of augmentation.

Given the distinct dynamics of EJPs within a burst noted in Diehl et al. (2013), we further examined EJP amplitudes within bursts across different inter-burst intervals. The intra-burst dynamics differed between $burst_1$ and $burst_{10}$, as demonstrated in an example recording of gm5b (Fig. 6A). As the dynamics were distinct early in the burst (Fig. 6A), the initial 10 EJPs in $burst_1$ and $burst_{10}$ for all intervals are presented for the three muscles (Fig. 6B,C). In $burst_1$, EJP_1 was small but EJP amplitude increased over the first several EJPs in all muscles (Fig. 6B). There appeared to be both summation of subsequent EJPs with previous ones and facilitation of EJP amplitude (Fig. 6B). In between trials (2–3 min), any plasticity decayed and the initial EJPs in $burst_1$ for all inter-burst intervals (2–32 s) overlapped, with the dynamics being similar across the three muscles (Fig. 6B). However, there were distinct amplitudes and dynamics of EJPs during the onset of $burst_{10}$ across different inter-burst intervals for all muscles (Fig. 6C). For instance, in gm8a and gm6ab, at a longer inter-burst interval such as 16 s, EJP_1 was smaller than later EJPs (Fig. 6C, green dashed lines). In response to 2 s inter-burst intervals, there was less difference in the amplitude of $burst_{10}$ EJP_1 relative to later EJPs (Fig. 6C, red dashed lines). The response of gm5b was different from those of gm8a and gm6ab. For example, at 16 s inter-burst intervals, $burst_{10}$ EJP_1 was similar in amplitude to subsequent EJPs (Fig. 6C, green dashed lines), while at 2 s inter-burst intervals, $burst_{10}$ EJP_1 was larger than subsequent EJPs, indicating that depression occurred. This is consistent with paired pulse data, which suggested a mix of depression and facilitation occurring in gm5b (also see below). The distinct relative amplitudes of EJP_1 and later EJPs in $burst_{10}$ versus those in $burst_1$ suggest that augmentation altered not only EJP amplitude across repeated bursts but also short-term facilitation/depression.

Interactions between facilitation and augmentation

To measure intra-burst dynamics during bursting activity that elicits different amounts of augmentation, the ratio of the last EJP to the first EJP (EJP_{last}/EJP_1) in $burst_{10}$ was measured across inter-burst intervals. In gm8a and gm6ab, at all inter-burst intervals the EJP_{last}/EJP_1 ratio was greater than 1, indicating facilitation (Fig. 7A,B,

Journal of Experimental Biology (2017) 220, 1233-1244 doi:10.1242/jeb.148908

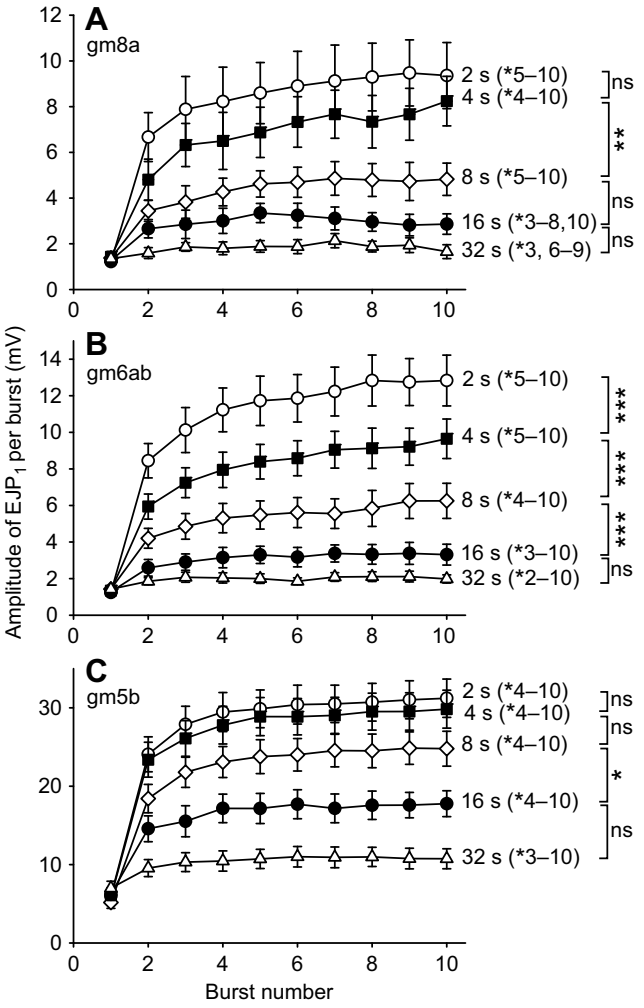

Fig. 4. Augmentation saturates at different inter-burst intervals for LG-innervated muscles. The amplitude of EJP_1 in each burst ($burst_{1–10}$) is plotted against burst number for different inter-burst intervals (2–32 s) for gm8a (A), gm6ab (B) and gm5b (C) (means±s.e.m). Symbols denote different inter-stimulus intervals, which are given to the right of all plots. Numbers in parentheses indicate the range of bursts in which EJP_1 amplitude was different from $burst_1$ EJP_1 [within muscle, multiple comparisons versus control group ($burst_1$, EJP_1), gm6ab and gm8a 32 s interval: one-way repeated measures ANOVA, Holm–Sidak *post hoc*; all other intervals: repeated measures ANOVA on ranks, Dunn's *post hoc*]. For simplicity in labeling, only *P*-values less than 0.05 are indicated, although some within each range were smaller. Brackets indicate differences between $burst_{6–10}$ EJP_1 in response to different inter-burst intervals within a muscle. Results are only indicated for neighboring intervals (gm8a and gm6ab: one-way repeated measures ANOVA, Holm–Sidak *post hoc*; gm5b: repeated measures ANOVA on ranks, Tukey *post hoc*). gm8a: n=9, N=4; gm6ab: n=12, N=6; gm5b: n=14, N=6. $^{*}P$<0.05, $^{***}P$<0.001, ^{ns}P>0.05.

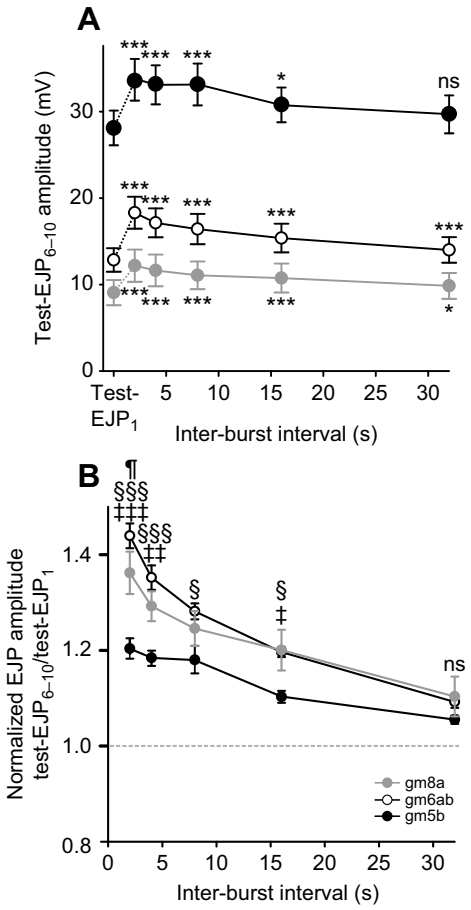

Fig. 5. The extent of augmentation differs across LG-innervated muscles. (A) Average test-$EJP_{6–10}$ amplitudes at different inter-burst intervals for gm8a, gm6ab and gm5b, with average test-EJP_1 amplitude plotted for reference [means±s.e.m; within muscle, multiple comparisons versus control group (test-EJP_1); gm6ab and gm8a: one-way repeated measures ANOVA, Holm–Sidak *post hoc*; gm5b: repeated measures ANOVA on ranks, Dunn's *post hoc*]. $^{***}P$<0.001, $^{*}P$<0.05, ^{ns}P>0.05. gm8a: n=9, N=4; gm6ab: n=12, N=6; gm5b: n=14, N=6. (B) Average test-$EJP_{6–10}$ amplitudes normalized to the average test-EJP_1 amplitudes (same symbols and n values as in A; means±s.e.m). The dashed gray line indicates no change in EJP amplitude (two-way ANOVA, Holm–Sidak *post hoc*). gm8a versus gm6ab: $^{¶}P$<0.05; gm8a versus gm5b: $^{‡‡‡}P$<0.001, $^{‡‡}P$<0.01, $^{‡}P$<0.05; gm6ab versus gm5b: $^{§§§}P$<0.001, $^{§}P$<0.05, ^{ns}P>0.05.

Table 1). However, in gm5b, the EJP_{last}/EJP_1 ratio was less than 1 at 2 and 4 s inter-burst intervals, indicating depression, not different from 1 at 8 s, suggesting a balance of facilitation and depression, and greater than 1 at all other intervals, indicating facilitation (Fig. 7C, Table 1). In all three muscles, there was a positive correlation between EJP_{last}/EJP_1 ratio and inter-burst interval (Fig. 7, Table 1). However, the slopes of these relationships were similar for gm8a and gm6ab, but different for gm5b (slope gm8a: 0.29; gm6ab: 0.34; gm5b: 0.06). More specifically, the EJP_{last}/EJP_1 ratios in gm8a and gm6ab were not different from each other, but the ratios in both gm8ab and gm6ab were greater than those in gm5b at inter-burst intervals of 8–32 s (Fig. 7D, Table 2). At 2 and 4 s intervals, depression occurred in gm5b but facilitation occurred in gm8a or gm6ab (Fig. 7). The intra-burst EJPs had an inter-stimulus interval of 100 ms. Although there was an indication of mixed depression and facilitation in the gm5b paired pulse data, facilitation always dominated, including at 100 ms paired inter-spike intervals (Fig. 2G). Thus, depression occurring during bursts of LG activity with inter-spike intervals of 100 ms highlights the complex manner in which synaptic transmission can be regulated by multiple forms of plasticity.

Summation

In addition to activity-dependent plasticity, other aspects of transmission at the neuromuscular junction can also shape the responses of muscles to motor neuron input. In particular, as evident in Figs 2, 3 and 6, a physiological LG firing frequency resulted in EJPs summating with previous EJPs. We therefore compared the decay time constants of the three muscles to determine whether summation was also a property that differed between these muscles. In overlaid traces, a gm5b EJP decayed more quickly than an EJP

Journal of Experimental Biology

Journal of Experimental Biology (2017) 220, 1233-1244 doi:10.1242/jeb.148908

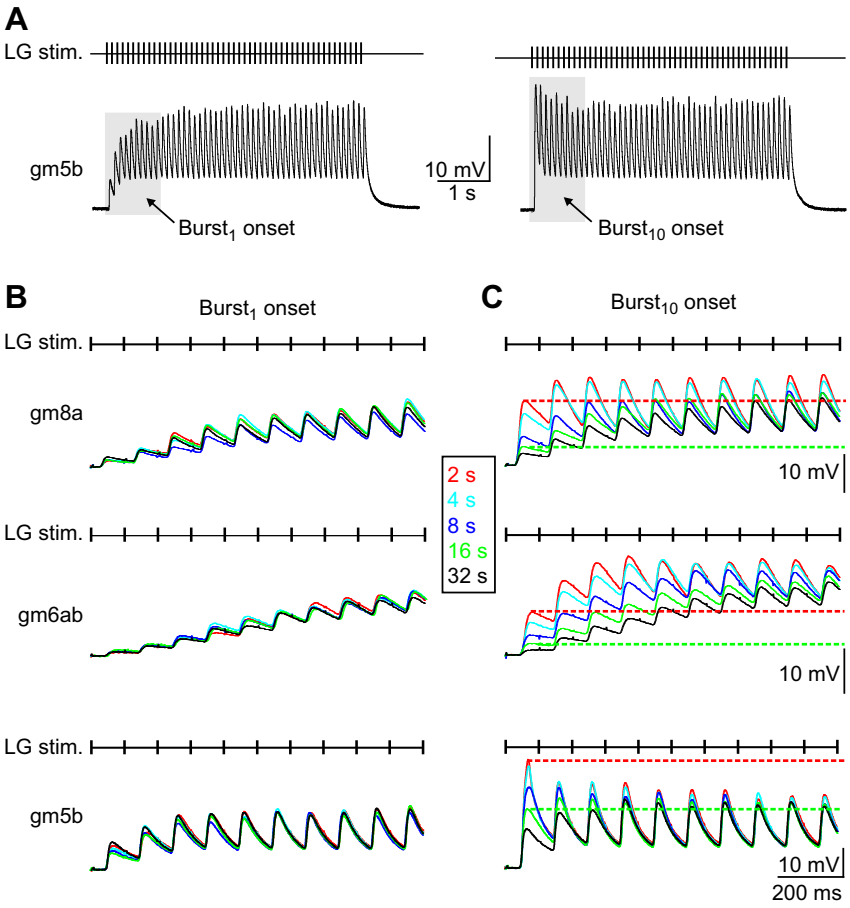

Fig. 6. Augmentation alters EJP dynamics. (A) Example recordings of $burst_1$ and $burst_{10}$ in gm5b highlight changes with repetitive bursts, particularly at the onset (gray boxes, expanded in B and C). (B) The first 10 EJPs in $burst_1$ in response to train stimulations with all five inter-burst intervals are overlaid for gm8a (top), gm6ab (middle) and gm5b (bottom). Box between traces indicates color key for inter-burst intervals. (C) The first 10 EJPs in $burst_{10}$ for the five inter-burst intervals are overlaid for gm8a (top), gm6ab (middle) and gm5b (bottom). Red dashed lines are drawn from the peak of EJP_1 for an inter-burst interval of 2 s, and the green dashed lines are drawn from the peak of EJP_1 for an inter-burst interval of 16 s for each muscle.

occurring in gm8a or gm6ab (Fig. 8A). This distinction was consistent across muscle fibers. The average decay time constant for gm8a and gm6ab did not differ (gm8a: 133.5±16.4 s; gm6ab: 134.8±12.6 s) (Fig. 8B, Table 2). However, the average decay time constant for gm5b EJPs (50.8±5.0 s) was different from that of gm8a and gm6ab (Fig. 8B, Table 2).

The effects of summation were examined in isolation from all other properties that were distinct between the muscles by using simulated EJPs (see Materials and methods), with the average time constants measured for the three muscles. In response to the stimulation pattern used to assay augmentation above, there was a larger amount of summation in gm8a and gm6ab relative to gm5b. Note the larger peak amplitude of the simulated EJP burst waveform for gm8a and gm6ab (Fig. 8C). However, EJPs fully decay even during the shortest inter-burst interval of 2 s used in this study (membrane potential returns to baseline before test pulse occurring 1.5 s after the burst; Fig. 8C). With only summation, there was no difference in simulated test-EJP amplitude from $burst_1$ to $burst_{10}$ for any inter-burst interval (test-$EJP_{6–10}$/test-EJP_1=1 for 2–32 s; Fig. 8D). Thus, the simulations indicate that summation shaped intra-burst EJP amplitudes with an LG firing frequency of 10 Hz, but across the physiological range of inter-burst intervals, summation does not contribute to shaping EJP responses.

DISCUSSION

This study identified augmentation as another form of synaptic plasticity that can differ at multiple synapses from the same motor neuron. This is an important form of synaptic plasticity in rhythmic behaviors such as locomotion, respiration and chewing, in which rhythmic motor neuron bursts are likely to induce augmentation. In the three target muscles of LG, multiple synaptic properties differed between muscles. Specifically, intra-burst facilitation/depression was regulated differently by the duration of inter-burst intervals between muscles. Additionally, there was less augmentation of EJP amplitude in gm5b, and augmentation saturated at longer inter-burst intervals in gm5b than in gm8a and gm6ab. Within bursts, muscle responses were also differentially shaped by summation, as a result of longer decay time constants in gm6ab and gm8a than in gm5b. Thus, there are distinctions between these muscles that are activity dependent on multiple time scales.

Physiological activity range

Inter-burst intervals in this study (2–32 s) encompass the range of inter-burst intervals recorded in LG *in vitro* and *in vivo* (2–24 s). The single firing rate (10 Hz=100 ms inter-spike interval) and burst duration (4.8 s) used were also within the physiological range of LG activity (inter-spike interval: 50–250 ms; burst duration: 2–9 s) (Beenhakker et al., 2004, 2005, 2007; Blitz et al., 2004b, 2008; Colton and Nusbaum, 2014; DeLong and Nusbaum, 2010; Diehl et al., 2013; Hedrich et al., 2011; Kirby and Nusbaum, 2007; White and Nusbaum, 2011). Thus, our data indicate that during gastric mill rhythms triggered by multiple inputs, augmentation and facilitation/depression would regulate responses of the three target muscles of LG. This is in agreement with the findings of Stein et al. (2006) in *C. pagurus*, that gm6ab is influenced by augmentation and facilitation during multiple versions of gastric mill rhythms.

The distinct facilitation/depression between the muscles, which is regulated by inter-burst interval duration, results in different

Journal of Experimental Biology (2017) 220, 1233-1244 doi:10.1242/jeb.148908

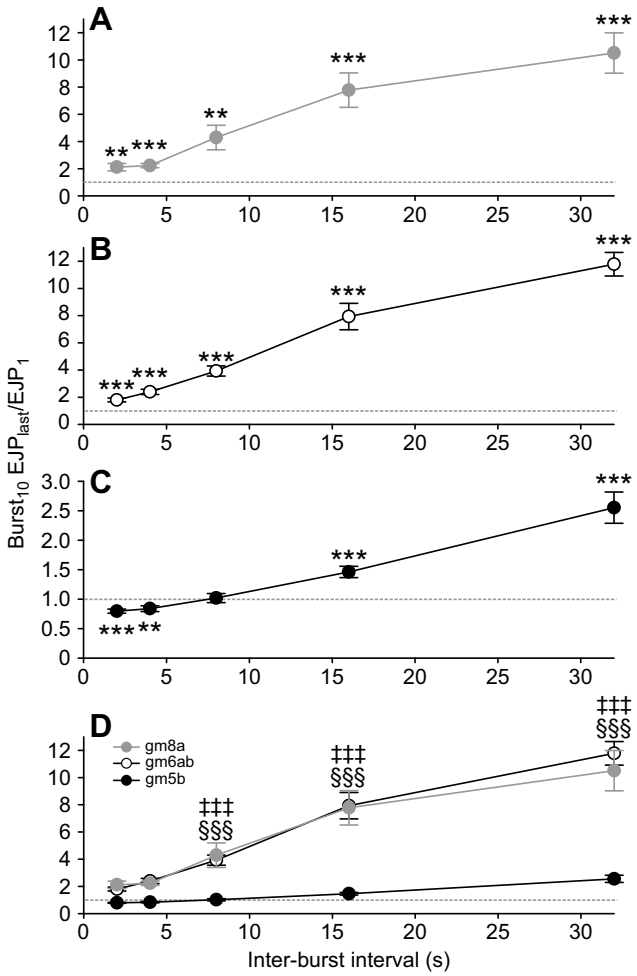

Fig. 7. Intra-burst facilitation correlates with inter-burst interval. (A–C) EJP_{last}/EJP_1 ratio in $burst_{10}$ at each interval for gm8a (A), gm6ab (B) and gm5b (C) (means±s.e.m). Dashed line indicates ratio of 1 (no facilitation or depression). ***P<0.001, **P<0.01 (one-sample t-test versus 1). (D) EJP_{last}/EJP_1 for gm8a, gm6ab and gm5b, overlaid to illustrate differences between muscles. ‡‡‡P<0.001 gm8a versus gm5b, §§§P<0.001 gm6ab versus gm5b (two-way ANOVA, Holm–Sidak *post hoc*). gm8a: n=9, N=4; gm6ab: n=12, N=6; gm5b: n=14, N=6.

dynamics throughout an LG burst. For instance, at the short end of the spectrum of physiological inter-burst intervals (3–4 s) (Beenhakker et al., 2004; Colton and Nusbaum, 2014; Diehl et al., 2013; Saideman et al., 2007), gm5b reached a peak depolarization with the first EJP, while gm6ab and gm8a depolarization increased over several EJPs even at 2 s. This could result in a faster rising phase of a gm5b contraction relative to the other LG innervated muscles. However, at long inter-burst intervals, such as those in response to proprioceptive feedback (~15–25 s) (DeLong and Nusbaum, 2010), gm5b EJPs undergo facilitation instead of depression. Thus, at these longer intervals, the gm5b muscle would likely also require multiple LG action potentials to reach a peak response, and result in similar contraction onset between the three LG innervated muscles. Further, because augmentation in gm5b saturates at longer inter-burst intervals than in gm6ab and gm8a, some changes (e.g. within 2–8 s inter-burst intervals) in LG activity could alter gm8a and gm6ab contraction strength with little impact on gm5b contraction strength. Augmentation regulates both the slope and peak of contractions in gm6ab measured in *C. pagurus* (Stein et al., 2006).

Contractions of LG muscles control movements in the gastric mill region of the foregut (Heinzel, 1988; Maynard and Dando, 1974; Weimann et al., 1991). There appear to be distinctions in their functions, with both gm6ab and gm8a pulling the two lateral teeth toward the midline for the power stroke of chewing, and gm5b involved in moving accessory teeth (Maynard and Dando, 1974). Comparing movements of the lateral teeth during two different chewing motor patterns, the time for the teeth to reach the midline and subsequently the time during which a maximum amount of tension is produced varies (Diehl et al., 2013). The focus of Diehl et al. (2013) was on the intra-burst timing of LG action potentials. However, it was also noted that there were distinct dynamics in the three LG muscles, but this was not pursued (Diehl et al., 2013). The mechanosensory-induced rhythm in which the teeth reach the midline more quickly also has a shorter inter-burst interval than the other rhythm (Diehl et al., 2013; White and Nusbaum, 2011). Thus, the greater augmentation and larger initial EJP amplitude in gm6ab and gm8a at shorter inter-burst intervals may contribute to a faster protraction of the lateral teeth toward the midline and a larger portion of the 'bite' being at maximum contraction.

The accessory teeth are positioned closer to the cardiopyloric valve than the main lateral and medial teeth. This valve enables chewed food to move from the gastric mill region containing the teeth to the pylorus containing the filtering apparatus. A potential role of gm5b control of the accessory teeth is to move chewed food toward the cardiopyloric valve and into the pylorus for filtering (Heinzel et al., 1993). At short inter-burst intervals, the large initial gm5b EJP amplitude may facilitate faster movement of residual chewed food toward the valve slightly ahead of the crushing action of the lateral teeth controlled by gm6ab and gm8a. The divergent control of gm8a/gm6ab (lateral teeth) and gm5b (accessory teeth) could contribute to efficient movement of chewed food toward the filtering region and clearing space for processing the next bolus of chewed food. This may be particularly important at shorter inter-burst intervals when there is less time between 'bites' for food to move through and thus gm5b has a large initial amplitude at shorter inter-burst intervals.

Differences between synaptic contacts from a single neuron

Short-term activity-dependent plasticity is mediated by both presynaptic and postsynaptic mechanisms. Presynaptically, residual Ca^{2+} in the axon terminal from the previous action potential can result in facilitation of release in response to a subsequent action potential, while vesicle depletion from the readily releasable vesicle pool can result in depression (Fioravante and Regehr, 2011; Martinez et al., 2014; Regehr, 2012). Additionally, postsynaptic mechanisms such as desensitization or saturation of postsynaptic receptors can contribute to decreased responses to subsequent stimuli (Blitz et al., 2004a; Regehr, 2012). We did not explore whether differences in short-term activity-dependent plasticity identified in this study are due to presynpatic or postsynaptic differences. However, in the lobster *Homarus americanus* STNS, the medial gastric motor neuron elicits distinct responses to burst stimulations in two target muscles. Distinctions include larger EJPs which depress at one target muscle, and smaller EJPs which summate and facilitate at another target muscle. Responses to repetitive bursting activity were not examined (Katz et al., 1993). In this study, differences in short-term plasticity appear to be dominated by presynaptic contributions, including anatomical differences in release sites. Additionally, postsynaptic contributions such as a longer time constant in the summating muscle shape distinct muscle responses (Katz et al., 1993). Other studies also

Journal of Experimental Biology (2017) 220, 1233-1244 doi:10.1242/jeb.148908

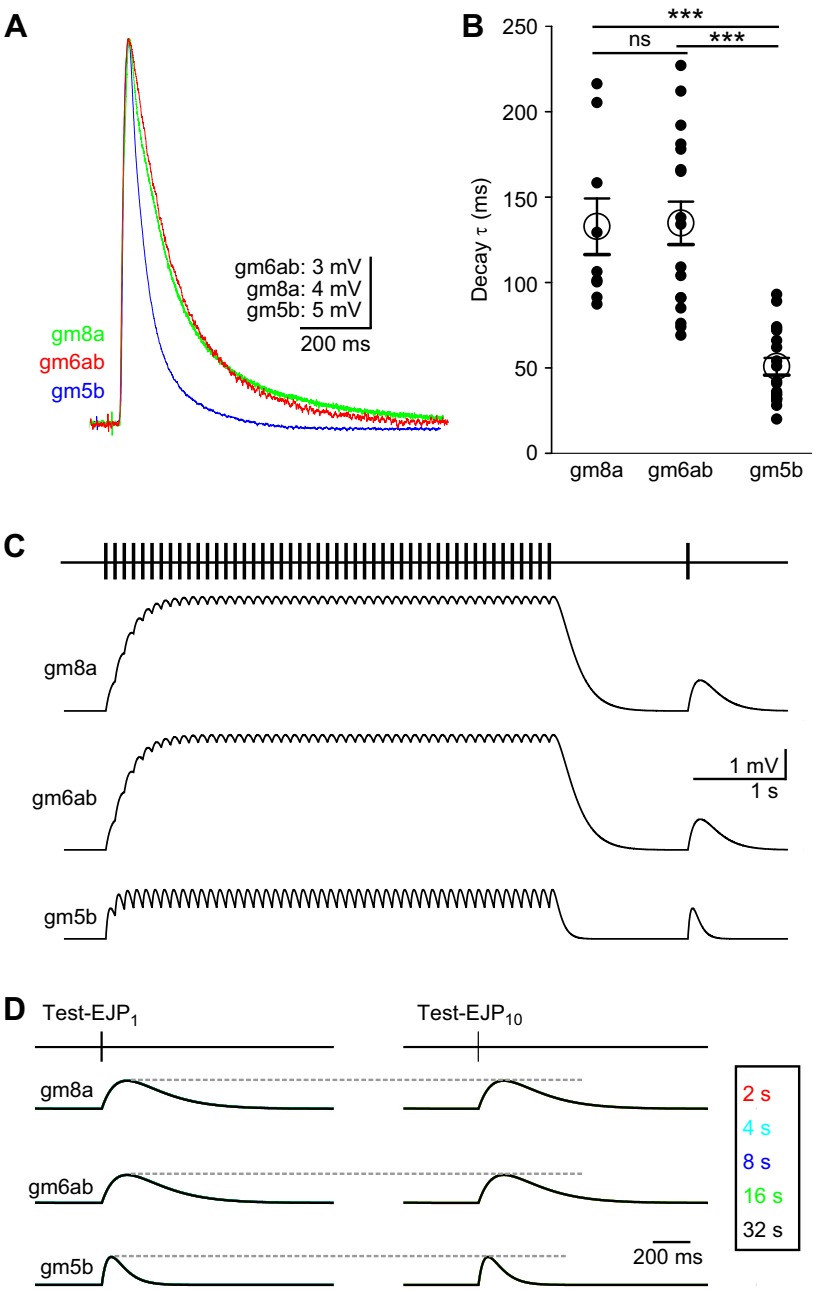

Fig. 8. Distinct decay time constants result in different extents of summation in LG-innervated muscles. (A) Single EJPs in gm8a, gm6ab and gm5b are overlaid. (B) The decay time constants (τ) for the three muscles in individual fibers (filled circles) and the means (±s.e.m.; large open circles) across each muscle (ANOVA on ranks, Dunn's *post hoc*). ***P<0.001, ^{ns}P>0.05. gm8a: n=9, N=4; gm6ab: n=17, N=11; gm5b: n=19, N=11. (C) EJPs were simulated (see Materials and methods) using the same stimulation protocol used for augmentation experiments. Simulated burst$_{10}$ with an inter-burst interval of 2 s using the average decay time constant for gm8a (top), gm6ab (middle) and gm5b (bottom) is displayed. A single EJP in all three muscles was scaled to the same amplitude. (D) Simulated test-EJP$_1$ and test-EJP$_{10}$ for all inter-burst intervals are overlaid with an inter-burst interval of 32 s at the forefront. The color code is indicated to the right; however, because of complete overlap in traces, only the 32 s trace at the forefront is visible. Dashed gray lines indicate the peak of test-EJP$_1$.

point to predominantly presynaptic mechanisms underlying differences in target cell-specific short-term plasticity (Blackman et al., 2013; Reyes et al., 1998; Scanziani et al., 1998). Although the functions may not yet be identified, distinct short-term plasticity at different presynaptic terminals of the same neuron suggests that this plasticity has specific functions appropriate for each target. This leads to a prediction that the postsynaptic neuron could play some role in determining plasticity. In fact, genetic manipulations at central and peripheral synapses indicate that retrograde signals from postsynaptic cells specifically regulate transmitter release from their partner presynaptic compartment (Blackman et al., 2013; Davis and Goodman, 1998). Thus, changes in presynaptic release probability may be the dominant means by which target cell-specific plasticity is determined. However, presynaptic differences at multiple synapses of a single neuron can develop in response to retrograde signals from postsynaptic targets.

The LG neuromuscular synapses express multiple forms of short-term plasticity simultaneously, similar to many other synapses. However, the balance of multiple forms of plasticity differs between synapses and in response to different activity patterns. For instance, facilitation tends to dominate at presynaptic terminals with low release probability, while depression is common at presynaptic terminals with high release probability (Blitz et al., 2004a; Martinez et al., 2014; Regehr, 2012; Zucker and Regehr, 2002). This may explain the switch from facilitation of gm5b EJPs to depression at shorter inter-burst intervals, during which augmentation likely increases release probability (Magleby and Zengel, 1976; Regehr, 2012). The shape of the PPR plot for gm5b suggested the possibility that both facilitation and depression were regulating EJP amplitude at very short inter-stimulus intervals, but depression only dominated within bursts having short inter-burst intervals. Similarly, at rat neocortical synapses, intra-burst facilitation occurs during stimulation protocols

Journal of Experimental Biology

that elicit augmentation, even in response to inter-stimulus intervals that do not elicit facilitation as paired stimuli (Thomson, 2000). A form of plasticity that is not readily apparent at a particular synapse may be masked by other forms (Kalkstein and Magleby, 2004; Regehr, 2012). Thus, gm6ab and gm8a may also express depression, but the balance with facilitation and augmentation under our experimental conditions may differ in these muscles compared with gm5b. Modulation, different motor neuron activity patterns, and experimental manipulations that alter release probability can switch short-term plasticity between facilitation and depression (Barrière et al., 2008; Mori et al., 2004; Regehr, 2012; Zhao et al., 2011).

The translation of motor neuron spiking activity to EJP amplitudes is just one aspect of the neuromuscular transform. Contractile properties are also commonly non-linear, and can have distinct dynamics relative to motor neuron spike timing (Brezina et al., 2000; Enoka and Fuglevand, 2001; Hooper and Weaver, 2000; Jorge-Rivera et al., 1998). Further, from presynaptic transmitter release to the regulation of contraction machinery, all aspects of the neuromuscular transform are subject to neuromodulation and thus can differ according to the behavioral state of the organism (Brezina, 2010; Brezina et al., 2000; Hooper and Weaver, 2000; Williams et al., 2013; Worden, 1998). Given the prevalence of neuromodulators acting on muscles, including in the STNS (Brezina, 2010; Fort et al., 2004; Hooper et al., 1999; Jorge-Rivera and Marder, 1996; Jorge-Rivera et al., 1998; Wali, 1985; Weimann et al., 1997; Worden, 1998; Wu and Cooper, 2012), it is possible that there are modulatory conditions in which the balance of depression and facilitation, and the properties of augmentation between the three muscles may converge. Similarly, relaxation kinetics are modulated, and the differences in summation between the three muscles could converge under a particular modulatory environment (Jing et al., 2010; Jorge-Rivera et al., 1998). Some inputs that activate gastric mill rhythms with distinct LG activity patterns also likely trigger hormonal release (Messinger et al., 2005) (D.M.B., unpublished observations). It will be interesting to determine whether coordinated peripheral and central modulation, such as that matching relaxation rate to rhythm speed in the *Aplysia* feeding system (Jing et al., 2010), changes synaptic plasticity to enable convergent responses of the LG muscles under some modulatory conditions.

Acknowledgements
We thank D. Bucher for the paired pulse analysis script.

Competing interests
The authors declare no competing or financial interests.

Author contributions
D.M.B., A.E.P., J.K.L. and A.T.W. conceived and designed the study; A.E.P., J.K.L. and A.T.W. performed experiments; D.M.B., A.E.P., J.K.L. and A.T.W. analyzed data; D.M.B. drafted the manuscript; D.M.B., A.E.P., J.K.L. and A.T.W. edited and provided critical revision of manuscript; all authors approved the final version of the manuscript.

Funding
This work was supported by National Science Foundation (grant IOS-1153417, D.M.B.), Miami University Undergraduate Summer Scholarship (A.E.P.) and Miami University Undergraduate Research Award (J.K.L. and A.T.W.).

References
Atwood, H. L. (1967). Variation in physiological properties of crustacean motor synapses. *Nature* **215**, 57-58.
Barrière, G., Tartas, M., Cazalets, J.-R. and Bertrand, S. S. (2008). Interplay between neuromodulator-induced switching of short-term plasticity at sensorimotor synapses in the neonatal rat spinal cord. *J. Physiol.* **586**, 1903-1920.
Beenhakker, M. P., Blitz, D. M. and Nusbaum, M. P. (2004). Long-lasting activation of rhythmic neuronal activity by a novel mechanosensory system in the crustacean stomatogastric nervous system. *J. Neurophysiol.* **91**, 78-91.
Beenhakker, M. P., DeLong, N. D., Saideman, S. R., Nadim, F. and Nusbaum, M. P. (2005). Proprioceptor regulation of motor circuit activity by presynaptic inhibition of a modulatory projection neuron. *J. Neurosci.* **25**, 8794-8806.
Beenhakker, M. P., Kirby, M. S. and Nusbaum, M. P. (2007). Mechanosensory gating of proprioceptor input to modulatory projection neurons. *J. Neurosci.* **27**, 14308-14316.
Blackman, A. V., Abrahamsson, T., Costa, R. P., Lalanne, T. and Sjöström, P. J. (2013). Target-cell-specific short-term plasticity in local circuits. *Front. Synaptic Neurosci.* **5**, 11.
Blitz, D. M., Foster, K. A. and Regehr, W. G. (2004a). Short-term synaptic plasticity: a comparison of two synapses. *Nat. Rev. Neurosci.* **5**, 630-640.
Blitz, D. M., Beenhakker, M. P. and Nusbaum, M. P. (2004b). Different sensory systems share projection neurons but elicit distinct motor patterns. *J. Neurosci.* **24**, 11381-11390.
Blitz, D. M., White, R. S., Saideman, S. R., Cook, A., Christie, A. E., Nadim, F. and Nusbaum, M. P. (2008). A newly identified extrinsic input triggers a distinct gastric mill rhythm via activation of modulatory projection neurons. *J. Exp. Biol.* **211**, 1000-1011.
Brezina, V. (2010). Beyond the wiring diagram: signalling through complex neuromodulator networks. *Philos. Trans. R. Soc. Lond. B Biol. Sci.* **365**, 2363-2374.
Brezina, V., Orekhova, I. V. and Weiss, K. R. (2000). The neuromuscular transform: the dynamic, nonlinear link between motor neuron firing patterns and muscle contraction in rhythmic behaviors. *J. Neurophysiol.* **83**, 207-231.
Briggman, K. L. and Kristan, W. B. (2008). Multifunctional pattern-generating circuits. *Annu. Rev. Neurosci.* **31**, 271-294.
Colton, G. F. and Nusbaum, M. P. (2014). Distinct microcircuit response to equivalent input from a full vs. partial projection neuron population. Society for Neuroscience meeting 2014, Washington DC. Abstract, 828.24.
Crider, M. E. and Cooper, R. L. (2000). Differential facilitation of high- and low-output nerve terminals from a single motoneuron. *J. Appl. Physiol.* **88**, 987-996.
Daur, N., Diehl, F., Mader, W. and Stein, W. (2012a). The stomatogastric nervous system as a model for studying sensorimotor interactions in real-time closed-loop conditions. *Front. Comput. Neurosci.* **6**, 13.
Daur, N., Bryan, A. S., Garcia, V. J. and Bucher, D. (2012b). Short-term synaptic plasticity compensates for variability in number of motor neurons at a neuromuscular junction. *J. Neurosci.* **32**, 16007-16017.
Daur, N., Nganguia, H., Nadim, F. and Bucher, D. (2015). Does axonal influence on the spike interval structure matter? Society for Neuroscience meeting 2015, Chicago IL. Abstract, 422.11.
Davis, G. W. and Goodman, C. S. (1998). Synapse-specific control of synaptic efficacy at the terminals of a single neuron. *Nature* **392**, 82-86.
DeLong, N. D. and Nusbaum, M. P. (2010). Hormonal modulation of sensorimotor integration. *J. Neurosci.* **30**, 2418-2427.
Deng, P.-Y. and Klyachko, V. A. (2011). The diverse functions of short-term plasticity components in synaptic computations. *Commun. Integr. Biol.* **4**, 543-548.
Dickinson, P. S. (2006). Neuromodulation of central pattern generators in invertebrates and vertebrates. *Curr. Opin. Neurobiol.* **16**, 604-614.
Diehl, F., White, R. S., Stein, W. and Nusbaum, M. P. (2013). Motor circuit-specific burst patterns drive different muscle and behavior patterns. *J. Neurosci.* **33**, 12013-12029.
Dittman, J. S., Kreitzer, A. C. and Regehr, W. G. (2000). Interplay between facilitation, depression, and residual calcium at three presynaptic terminals. *J. Neurosci.* **20**, 1374-1385.
Dobrunz, L. E., Huang, E. P. and Stevens, C. F. (1997). Very short-term plasticity in hippocampal synapses. *Proc. Natl. Acad. Sci.* **94**, 14843-14847.
Doi, A. and Ramirez, J.-M. (2008). Neuromodulation and the orchestration of the respiratory rhythm. *Respir. Physiol. Neurobiol.* **164**, 96-104.
Enoka, R. M. and Fuglevand, A. J. (2001). Motor unit physiology: some unresolved issues. *Muscle Nerve* **24**, 4-17.
Fioravante, D. and Regehr, W. G. (2011). Short-term forms of presynaptic plasticity. *Curr. Opin. Neurobiol.* **21**, 269-274.
Fort, T. J., Brezina, V. and Miller, M. W. (2004). Modulation of an integrated central pattern generator–effector system: dopaminergic regulation of cardiac activity in the blue crab *Callinectes sapidus*. *J. Neurophysiol.* **92**, 3455-3470.
Geier, C. F. and Hooper, S. L. (2002). Modeling p1 (LP neuron) muscle isometric motor activity. Society for Neuroscience meeting 2002, Orlando FL, Abstract 465.9.
Harris-Warrick, R. M. (2011). Neuromodulation and flexibility in central pattern generator networks. *Curr. Opin. Neurobiol.* **21**, 685-692.
Hedrich, U. B. S., Diehl, F. and Stein, W. (2011). Gastric and pyloric motor pattern control by a modulatory projection neuron in the intact crab *Cancer pagurus*. *J. Neurophysiol.* **105**, 1671-1680.
Heinzel, H. G. (1988). Gastric mill activity in the lobster. I. Spontaneous modes of chewing. *J. Neurophysiol.* **59**, 528-550.
Heinzel, H. G., Weimann, J. M. and Marder, E. (1993). The behavioral repertoire of the gastric mill in the crab, *Cancer pagurus*: an in situ endoscopic and electrophysiological examination. *J. Neurosci.* **13**, 1793-1803.

Hooper, S. L. and Weaver, A. L. (2000). Motor neuron activity is often insufficient to predict motor response. *Curr. Opin. Neurobiol.* **10**, 676-682.
Hooper, S. L., Brezina, V., Cropper, E. C. and Weiss, K. R. (1999). Flexibility of muscle control by modulation of muscle properties. In *Beyond Neurotransmission: Neuromodulation and its Importance for Information Processing* (ed. P. S. Katz), pp. 241-275. Oxford University Press: Oxford.
Hooper, S. L., Guschlbauer, C., von Uckermann, G. and Büschges, A. (2007). Different motor neuron spike patterns produce contractions with very similar rises in graded slow muscles. *J. Neurophysiol.* **97**, 1428-1444.
Jing, J., Sweedler, J. V., Cropper, E. C., Alexeeva, V., Park, J.-H., Romanova, E. V., Xie, F., Dembrow, N. C., Ludwar, B. C., Weiss, K. R. et al. (2010). Feedforward compensation mediated by the central and peripheral actions of a single neuropeptide discovered using representational difference analysis. *J. Neurosci.* **30**, 16545-16558.
Jorge-Rivera, J. C. and Marder, E. (1996). TNRNFLRFamide and SDRNFLRFamide modulate muscles of the stomatogastric system of the crab *Cancer borealis*. *J. Comp. Physiol. A* **179**, 741-751.
Jorge-Rivera, J. C., Sen, K., Birmingham, J. T., Abbott, L. F. and Marder, E. (1998). Temporal dynamics of convergent modulation at a crustacean neuromuscular junction. *J. Neurophysiol.* **80**, 2559-2570.
Kalkstein, J. M. and Magleby, K. L. (2004). Augmentation increases vesicular release probability in the presence of masking depression at the frog neuromuscular junction. *J. Neurosci.* **24**, 11391-11403.
Katz, P. S., Kirk, M. D. and Govind, C. K. (1993). Facilitation and depression at different branches of the same motor axon: Evidence for presynaptic differences in release. *J. Neurosci.* **13**, 3075-3089.
Kirby, M. S. and Nusbaum, M. P. (2007). Peptide hormone modulation of a neuronally modulated motor circuit. *J. Neurophysiol.* **98**, 3206-3220.
Magleby, K. L. and Zengel, J. E. (1976). Augmentation: a process that acts to increase transmitter release at the frog neuromuscular junction. *J. Physiol.* **257**, 449-470.
Marder, E. and Bucher, D. (2007). Understanding circuit dynamics using the stomatogastric nervous system of lobsters and crabs. *Annu. Rev. Physiol.* **69**, 291-316.
Martinez, D., Matveev, V. and Nadim, F. (2014). Short-term synaptic plasticity in central pattern generators. In *Encyclopedia of Computational Neuroscience* (ed. D. Jaeger and R. Jung), pp. 1-14. New York: Springer.
Maynard, D. M. and Dando, M. R. (1974). The structure of the stomatogastric neuromuscular system in *Callinectes sapidus*, *Homarus americanus* and *Panulirus argus* (Decapoda Crustacea). *Philos. Trans. R. Soc. Lond. B Biol. Sci.* **268**, 161-220.
Messinger, D. I., Kutz, K. K., Le, T., Verley, D. R., Hsu, Y.-W., Ngo, C. T., Cain, S. D., Birmingham, J. T., Li, L. and Christie, A. E. (2005). Identification and characterization of a tachykinin-containing neuroendocrine organ in the commissural ganglion of the crab *Cancer productus*. *J. Exp. Biol.* **208**, 3303-3319.
Mori, M., Abegg, M. H., Gähwiler, B. H. and Gerber, U. (2004). A frequency-dependent switch from inhibition to excitation in a hippocampal unitary circuit. *Nature* **431**, 453-456.
Morris, L. G. and Hooper, S. L. (1997). Muscle response to changing neuronal input in the lobster (*Panulirus interruptus*) stomatogastric system: spike number- versus spike frequency-dependent domains. *J. Neurosci.* **17**, 5956-5971.
Morris, L. G. and Hooper, S. L. (1998). Muscle response to changing neuronal input in the lobster (*Panulirus interruptus*) stomatogastric system: slow muscle properties can transform rhythmic input into tonic output. *J. Neurosci.* **18**, 3433-3442.
Nusbaum, M. P. and Beenhakker, M. P. (2002). A small-systems approach to motor pattern generation. *Nature* **417**, 343-350.
Regehr, W. G. (2012). Short-term presynaptic plasticity. *Cold Spring Harb. Perspect. Biol.* **4**, a005702.
Reyes, A., Lujan, R., Rozov, A., Burnashev, N., Somogyi, P. and Sakmann, B. (1998). Target-cell-specific facilitation and depression in neocortical circuits. *Nat. Neurosci.* **1**, 279-285.
Saideman, S. R., Blitz, D. M. and Nusbaum, M. P. (2007). Convergent motor patterns from divergent circuits. *J. Neurosci.* **27**, 6664-6674.
Scanziani, M., Gähwiler, B. H. and Charpak, S. (1998). Target cell-specific modulation of transmitter release at terminals from a single axon. *Proc. Natl. Acad. Sci.* **95**, 12004-12009.
Sen, K., Jorge-Rivera, J. C., Marder, E. and Abbott, L. F. (1996). Decoding synapses. *J. Neurosci.* **16**, 6307-6318.
Stein, W. (2009). Modulation of stomatogastric rhythms. *J. Comp. Physiol. A Neuroethol. Sens. Neural Behav. Physiol* **195**, 989-1009.
Stein, W., Smarandache, C. R., Nickmann, M. and Hedrich, U. B. S. (2006). Functional consequences of activity-dependent synaptic enhancement at a crustacean neuromuscular junction. *J. Exp. Biol.* **209**, 1285-1300.
Thomson, A. M. (2000). Facilitation, augmentation and potentiation at central synapses. *Trends Neurosci.* **23**, 305-312.
Wali, F. A. (1985). Actions of polypeptides at the neuromuscular junction. *Agents Actions* **16**, 558-566.
Weimann, J. M., Meyrand, P. and Marder, E. (1991). Neurons that form multiple pattern generators: identification and multiple activity patterns of gastric/pyloric neurons in the crab stomatogastric system. *J. Neurophysiol.* **65**, 111-122.
Weimann, J. M., Skiebe, P., Heinzel, H. G., Soto, C., Kopell, N., Jorge-Rivera, J. C. and Marder, E. (1997). Modulation of oscillator interactions in the crab stomatogastric ganglion by crustacean cardioactive peptide. *J. Neurosci.* **17**, 1748-1760.
White, R. S. and Nusbaum, M. P. (2011). The same core rhythm generator underlies different rhythmic motor patterns. *J. Neurosci.* **31**, 11484-11494.
Williams, A. H., Calkins, A., O'Leary, T., Symonds, R., Marder, E. and Dickinson, P. S. (2013). The neuromuscular transform of the lobster cardiac system explains the opposing effects of a neuromodulator on muscle output. *J. Neurosci.* **33**, 16565-16575.
Worden, M. K. (1998). Modulation of vertebrate and invertebrate neuromuscular junctions. *Curr. Opin. Neurobiol.* **8**, 740-745.
Wu, W.-H. and Cooper, R. L. (2012). Serotonin and synaptic transmission at invertebrate neuromuscular junctions. *Exp. Neurobiol.* **21**, 101-112.
Zhao, S., Sheibanie, A. F., Oh, M., Rabbah, P. and Nadim, F. (2011). Peptide neuromodulation of synaptic dynamics in an oscillatory network. *J. Neurosci.* **31**, 13991-14004.
Zhurov, Y. and Brezina, V. (2006). Variability of motor neuron spike timing maintains and shapes contractions of the accessory radula closer muscle of *Aplysia*. *J. Neurosci.* **26**, 7056-7070.
Zoccolan, D., Pinato, G. and Torre, V. (2002). Highly variable spike trains underlie reproducible sensorimotor responses in the medicinal leech. *J. Neurosci.* **22**, 10790-10800.
Zucker, R. S. and Regehr, W. G. (2002). Short-term synaptic plasticity. *Annu. Rev. Physiol.* **64**, 355-405.